Synthesis and Characterization of Ferrocenyl-Modified Mesoporous Silicates

ARTICLE *in* CHEMISTRY OF MATERIALS · NOVEMBER 1998

Impact Factor: 8.35 · DOI: 10.1021/cm980510g

6 AUTHORS, INCLUDING:

Stephen O'Brien
City College of New York
126 PUBLICATIONS **7,787** CITATIONS
SEE PROFILE

Stephen Barlow
Georgia Institute of Technology
284 PUBLICATIONS **11,492** CITATIONS
SEE PROFILE

Dermot O'Hare
University of Oxford
392 PUBLICATIONS **10,308** CITATIONS
SEE PROFILE

Synthesis and Characterization of Ferrocenyl-Modified Mesoporous Silicates

Stephen O'Brien, Julian M. Keates, Stephen Barlow, Mark J. Drewitt, Benjamin R. Payne, and Dermot O'Hare*

Inorganic Chemistry Laboratory, University of Oxford, South Parks Road, Oxford, OX1 3QR, UK

Received July 20, 1998. Revised Manuscript Received September 25, 1998

The mesoporous silicates MCM-41 and FSM-16 have been functionalized with a range of ferrocenyl groups. The general synthetic methodology involves either reaction of the strained [1]ferrocenophanes [Fe(η-C_5R_4)$_2$SiMe$_2$] (R = H or Me), [Fe(η-C_9Me_6)(η-C_5H_4)SiMe$_2$], or the ferrocenyl carbocation [Fe(η-C_5Me_5)(η-$C_5Me_4CH_2$)]$^+$ with the dehydrated mesoporous silicate. The materials have been extensively characterized by (inter alia) solid-state ^{13}C and ^{29}Si NMR and Fe K-edge EXAFS spectroscopy. The reaction of either [Fe(η-C_5H_4)$_2$SiMe$_2$] or [Fe(η-C_5Me_4)$_2$SiMe$_2$] with MCM-41 affords both single ferrocenyl and short chain oligo(ferrocenyl) units grafted to the silicate walls of the mesopores. In contrast, the reaction of [Fe(η-C_9Me_5)(η-C_5H_4)SiMe$_2$] with MCM-41 gives only a single type of ferrocenyl group attached to the pore walls via a regiospecific ring-opening reaction in which the Si−(C_5H_4) bond is broken in preference to the Si−(C_9Me_6) bond.

Introduction

The synthesis, characterization, and potential uses of the new generation of mesoporous silicates are well-established.[1] Among the materials described, characterized, and classified are hexagonal (*P*6*mm*) MCM-41[2,3] and FSM-16, derived from intercalation of alkyltrimethylammonium cations into a layered polysilicate.[4,5] The size and regularity of the channels in mesoporous silicates (uniform pore diameters of 20−100 Å, and recently up to 300 Å)[6] allow the inclusion of substrates much larger than previously possible using zeolites as hosts (pore diameters in the range 3−10 Å). To create a material with specific catalytic, adsorptive, or sensing properties, the interior of the mesopores may be modified by chemical methods. The immobilization of transition metal catalysts by chemical attachment to the reactive hydroxyl groups within the large internal surface area of the mesoporous silicate (in MCM-41 an estimated 8−27% of the silicon atoms have pendant OH groups)[7] is one such method. The nature and density of surface silanol (Si−OH) groups present have already received much attention. It can be expected that the surface behavior is very similar to that of high surface area amorphous silica. Investigations of hydroxylated silica materials indicated that four or five Si−OH groups per square nanometer remain after drying at 120−150 °C. The average Si(OH)−Si(OH) distance determined by experiment is ∼7 Å.[2,8] For FSM-16, Ishikawa et al. determined the surface silanol density to be 3.3 Si−OH nm^{-2}, notably lower than for other silicas.[7]

One problem associated with pore modification of mesoporous silicates is the difficulty in obtaining sufficient characterizing data to determine the species present. Another issue is whether they are active within the channels of the host structure. Bein and co-workers reported the grafting of a trimethylstannyl moiety onto MCM-41,[9] while Thomas and co-workers achieved the inclusion of catalytically active (≡SiO)$_3$TiOH units inside the channels of MCM-41, using [Ti(η-C_5H_5)$_2$-Cl_2] as a precursor.[10,11] In these studies, extended X-ray absorption fine structure (EXAFS) spectroscopy was used extensively to identify the change in environment of the metal center as a result of thermolysis. We have previously employed EXAFS spectroscopy in order to characterize a chiral olefin polymerization catalyst incorporated in MCM-41 modified with methylalumoxane.[12] Stucky and co-workers reported the immobilization of $O_{3/2}V{=}O$ centers on cubic MCM-48.[13] Wide-line solid-state ^{51}V NMR and UV−vis spectroscopy provided

(1) Beck, J. S.; Vartuli, J. C. *Curr. Opin. Solid State Mater. Sci.* **1996**, *1*, 76−87.
(2) Beck, J. S.; Vartuli, J. C.; Roth, W. J.; Leonowicz, M. E.; Kresge, C. T.; Schmitt, K. D.; Chu, C. T. W.; Olson, D. H.; Sheppard, E. W.; Mccullen, S. B.; Higgins, J. B.; Schlenker, J. L. *J. Am. Chem. Soc.* **1992**, *114*, 10834−10843.
(3) Vartuli, J. C.; Schmitt, K. D.; Kresge, C. T.; Roth, W. J.; Leonowicz, M. E.; Mccullen, S. B.; Hellring, S. D.; Beck, J. S.; Schlenker, J. L.; Olson, D. H.; Sheppard, E. W. *Chem. Mater.* **1994**, *6*, 2317−2326.
(4) Inagaki, S.; Fukushima, Y.; Kuroda, K. *J. Chem. Soc., Chem. Commun.* 1993, 680−682.
(5) Inagaki, S.; Koiwai, A.; Suzuki, N.; Fukushima, Y.; Kuroda, K. *Bull. Chem. Soc. Jpn.* **1996**, *69*, 1449−1457.
(6) Zhao, D. Y.; Feng, J. L.; Huo, Q. S.; Melosh, N.; Fredrickson, G. H.; Chmelka, B. F.; Stucky, G. D. *Science* **1998**, *279*, 548−552.
(7) Ishikawa, T.; Matsuda, M.; Yasukawa, A.; Kandori, K.; Inagaki, S.; Fukushima, T.; Kondo, S. *J. Chem. Soc., Faraday Trans.* **1996**, *92*, 1985−1989.
(8) Chen, C.-Y.; Burkett, S. L.; Davis, M. E.; Li, H. X. *Micoporous Mater.* **1993**, *2*, 1−17.
(9) Huber, C.; Moller, K.; Bein, T. *J. Chem. Soc. Chem. Commun.* **1994**, 2619−2620.
(10) Maschmeyer, T.; Rey, F.; Sankar, G.; Thomas, J. M. *Nature* **1995**, *378*, 159−162.
(11) Sinclair, P. E.; Sankar, G.; Catlow, C. R. A.; Thomas, J. M.; Maschmeyer, T. *J. Phys. Chem. B* **1997**, *101*, 4232.
(12) O'Brien, S.; Tudor, J.; Maschmeyer, T.; O'Hare, D. *Chem. Commun.* **1997**, 1905.

10.1021/cm980510g CCC: $15.00
Published on Web 11/12/1998

evidence for a pseudotetrahedral (rather than octahedral) environment of the V atoms in dehydrated samples by comparison with other V/SiO_2 materials. The proposed structure exhibits a vanadyl (V═O) moiety anchored to the surface of the pore wall via three Si−O−V bridges.

The functionalization of silica surfaces with (1,1′-ferrocenediyl)dimethylsilane, first reported by Wrighton and co-workers,[14] utilized the susceptibility of the strained C−Si−C bridge to nucleophilic attack by the hydroxyl groups on the surface of the silica wall. It has been previously observed that reaction of [1]ferrocenophanes with nucleophiles can lead to oligomeric and higher molecular weight species.[15,16] We recently reported that (1,1′-ferrocenediyl)dimethylsilane could be grafted onto the walls of MCM-41.[17] MacLachlan et al. found that with higher loadings of (1,1′-ferrocenediyl)dimethylsilane achieved by a vapor phase method, thermal ring-opening polymerization (TROP) could also be carried out within the pores of MCM-41.[18]

Here we report more fully on the use of ring-opening reactions of the strained [1]ferrocenophanes [Fe(η-$C_5R_4)_2SiMe_2$] (R = H or Me) and [Fe(η-C_9Me_6)(η-C_5H_4)-$SiMe_2$] as a low-temperature, high-yield method of functionalizing the mesoporous silicates MCM-41 and FSM-16. The nature of the organometallic moieties within these materials has been studied in detail using solid-state ^{13}C and ^{29}Si NMR and Fe K-edge EXAFS spectroscopy.

Experimental Details

General. All air-sensitive reactions and manipulations were routinely performed under a nitrogen atmosphere by using standard Schlenk techniques. Solvents were dried by reflux over the appropriate drying agent, distilled under nitrogen, and stored in Young's-type or RotoFlo ampules. X-ray powder diffraction data were recorded on a Siemans D5000 diffractometer, using monochromated Cu Kα (λ = 1.54056 Å) radiation at 40 kV and 30 mA. Fourier transform infrared spectra were recorded on a Perkin-Elmer FT-1710 spectrometer. High-resolution transmission electron microscopy and electron diffraction experiments were performed on a JEOL 2010 electron microscope operating at 200 kV.

Solid-State NMR Spectroscopic Experiments. The solid-state ^{13}C and ^{29}Si NMR spectra were obtained on a Bruker MSL-200 spectrometer equipped with an Oxford Instruments 4.7 T superconducting cryomagnet operating at Zeeman frequencies of 200.13 MHz for ^1H, 50.32 MHz for ^{13}C, and 39.76 MHz for ^{29}Si. Spectra were acquired using either a Bruker HP 73A MAS 7DB or MAS-7BB-HT probe. Magic angle spinning (MAS) was employed for all ^{29}Si and ^{13}C experiments at spinning rates of 2.47−3.30 and 2.66−3.40 kHz, respectively. Contact times were typically 1−2 ms with recycle delays of 2−3 s. All samples were packed into 7 mm o.d. zirconia rotors fitted with Kel-F or BN caps and spun with dry N_2. For air-sensitive compounds, samples were packed into Kel-F inserts in a N_2 glovebox and then inserted into the zirconia rotors. Chemical shifts were referenced to kaolinite for ^{29}Si (δ = −91.5) and adamantane for ^{13}C (δ = 29.5, low-frequency resonance) as secondary external standards. Low-temperature ^{13}C experiments were performed using a Bruker BVT-100 VT unit.

EXAFS Data Acquisition and Analysis. EXAFS experiments were performed at the CLRC Daresbury Laboratory, Cheshire, UK, with the storage ring operating in multibunch mode (2 GeV) with typical currents of 180−250 mA. Fe K-edge transmission and fluorescence EXAFS were recorded at room temperature on Station 8.1. Typically, scans were set up to record the pre-edge at 5 eV steps, the absorption edge at 0.5 eV steps, and the post-edge region in 0.06−0.08 $Å^{-1}$ steps, giving a total acquisition time of ca. 40 min per scan. A double crystal monochromator in a nondispersive configuration equipped with flat Si (220) crystals (giving 50% harmonic rejection) was used with an entrance slit ca. 3 mm wide and 1 mm high. Data were collected in transmission mode and calibrated against an Fe foil of thickness 50 mm (energy of Fe K-edge, metal = 7110.8 eV). Detectors were filled with Ar, 20% absorbing I_0 (incidence) and 80% absorbing I_t (transmission). Samples were typically diluted with MgO and compressed to a disk of 1−2 mm thickness using a pellet press. Data analysis of the EXAFS was performed according to standard procedures. The Fe K-edge of the X-ray absorption spectrum was calibrated using the EXCALIB program and background subtraction was performed with EXBACK (part of the EXAFS suite of software available at Daresbury laboratory), using a smoothing spline ranging from ca. 20 eV above the edge to the end of the usable part of the spectrum, ca. 600 eV beyond the edge, with a multiple polynominal fit (two coupled polynomials). The EXAFS structural parameters [shell radius (R), Debye−Waller factors ($A = 2\sigma^2$), coordination number (N), phase (p), and E_o value] were varied in the multiple-shell curve fitting program EXCURV92. The value of E_o was also permitted to vary to allow for inaccuracies incurred in the potential calculations and in the setting of E_o during background subtraction.

Synthesis of FSM-16. A sodium silicate solution (Na/Si mole ratio = 1:1, 15 wt % in water) was heated in a platinum crucible from 100 to 750 °C at a rate of 5 °C min^{-1} and then maintained at 750 °C for 1 h. The product was δ-$Na_2Si_2O_5$, a bright white solid of porous appearance. Kanemite ($NaHSi_2O_5 \cdot 3H_2O$) was made by suspending δ-$Na_2Si_2O_5$ (5 g, 27 mmol) in deionized water (100 mL), followed by stirring at room temperature for exactly 30 min. The X-ray diffraction patterns of powdered samples of both silicates were in agreement with literature values.[19−21] A solid-state ^{29}Si CP MAS NMR spectrum of kanemite exhibited a single isotropic peak at δ = −97.0 [fwhm ($\nu_{1/2}$) = 27.6 Hz].

The silicate−organic complex was prepared by stirring a mixture of kanemite (1 g) and a 0.1 mol dm^{-3} solution of cetyltrimethylammonium chloride (20 mL, C_{16}TMACl; kanemite/C_{16}TMACl = 2.2) at 70 °C for 3 h. Elemental analysis at this stage indicated 46.7 wt % organic content. X-ray diffraction powder pattern reflections were observed at d spacings of 38.0, 30.5, 28.0, 21.9, 19.0, 15.0, and 14.1 Å. A ^{29}Si MAS NMR spectrum exhibited broad resonances at δ = −89.6 (trace Q_2), −99.5 (Q_3), and −109.1 (Q_4). After cooling to room temperature, the mixture was centrifuged three times to remove dissolved silica followed by dispersion of the solid product in deionized water. The pH of the suspension was slowly lowered to 8.5 by the dropwise addition of 2 M HCl over 18 h. The resultant white product was filtered, washed with deionized water (3 × 100 mL), and dried in air to yield a silicate−organic complex. Elemental analysis: C, 40.2; N 2.45; H 8.4. Integration of a ^{29}Si MAS NMR spectrum gave a Q_4:Q_3 ratio of 1:3. Calcination (540 °C, 5 °C min^{-1} ramp, 8 h dwell) of the silicate−organic complex afforded FSM-16: surface area

(13) Morey, M.; Davidson, A.; Eckert, H.; Stucky, G. *Chem. Mater.* **1996**, *8*, 486-492.
(14) Fischer, A. B.; Kinney, J. B.; Staley, R. H.; Wrighton, M. S. *J. Am. Chem. Soc.* **1979**, *101*, 6501−6506.
(15) Withers, H. P.; Seyferth, D.; Fellman, J. D.; Garrou, P. E.; Martin, S. *Organometallics* **1982**, *1*, 1283−1288.
(16) Rulkens, R.; Lough, A. J.; Manners, I. *J. Am. Chem. Soc.* **1994**, *116*, 797.
(17) O'Brien, S.; Tudor, J.; Barlow, S.; Drewitt, M. J.; Heyes, S. J.; O'Hare, D. *Chem. Commun.* **1997**, 641.
(18) MacLachlan, M. J.; Aroca, P.; Coombs, N.; Manners, I.; Ozin, G. A. *Adv. Mater.* **1998**, *10*, 144.
(19) Williamson, J.; Glasser, F. P. *Phys. Chem. Glasses* **1966**, *7*, 127−138.
(20) Johan, Z.; Maglione, G. F. *Bull. Soc. Fr. Minéral. Cristallogr.* **1972**, *95*, 371−382.
(21) Beneke, K.; Lagaly, G. *Am. Mineral.* **1977**, *62*, 763.

Figure 1. Transmission electron micrograph (inset: electron diffraction pattern) of FSM-16.

(N_2 BET), 960 $m^2\ g^{-2}$; estimated average pore diameter, 2.7 nm; X-ray diffraction powder pattern reflections observed at *d* spacings of 37.5, 21.6, 18.7, and 14.1 Å. A ^{29}Si MAS NMR spectrum indicated a greatly increased Q_4:Q_3 ratio. The transmission electron micrograph (TEM) of the calcined product (Figure 1) clearly illustrates the periodic order of the hexagonal mesopores.

Synthesis of MCM-41. MCM-41 was prepared according to literature methods.[2,22] A 29 wt % hydroxide-exchanged cetyltrimethylammonium chloride surfactant solution (C_{16}TMACl^-/OH^-, 30 wt % OH) was prepared by passing a 25 wt % solution of C_{16}TMACl through an ion exchange column (DOWEX, IRA-100, Aldrich) four or five times followed by eluting with deionized water until the pH of the eluant was 7.0. The dilute solution was then concentrated by heating to give the required weight percent. MCM-41 was synthesized by mixing the 29 wt % solution of C_{16}TMACl^-/OH^- (4.41 g, 4 mmol) with a tetramethylammonium (TMA)−silicate solution prepared from TMAOH (40 wt % TMAOH solution, 0.93 g, 4 mmol), fumed SiO_2 (Aldrich, 0.858 g, 14.3 mmol), Al_2O_3 (0.05 g, 0.5 mmol), and deionized H_2O (1.75 g, 9.7 mmol). The resulting white gel was stirred for 1 h at room temperature and then heated at 150 °C for 2 days in a steel autoclave. The solid phase was recovered by filtration, washed several times with deionized water, and then air-dried over several days. Calcination in air (700 °C, 5 °C min^{-1} ramp, 6 h dwell) afforded a powdery white solid: surface area (N_2 BET), 900 $m^2\ g^{-2}$; estimated pore diameter, 3.0 nm; X-ray diffraction powder pattern reflections observed at *d* spacings of 38.0, 21.9, 19.0, and 14.2 Å.

Synthesis of MCM-41/Fe(C_5H_4)$_2$SiMe$_2$ (1). [Fe(η-C_5H_4)$_2$SiMe$_2$] was synthesized by reaction of the TMEDA adduct of dilithioferrocene and Me_2SiCl_2 in pentane and was purified by vacuum sublimation.[14] MCM-41 (200 mg) was heated to 150 °C under a dynamic vacuum of 10^{-4} Torr for 6 h. [Fe(η-C_5H_4)$_2$SiMe$_2$] (150 mg) was dissolved in dry pentane (40 mL) and transferred onto the MCM-41. The slurry was stirred for 24 h under N_2. The slurry was allowed to settle and the supernatant decanted. The resulting air stable orange powder (330 mg) was washed repeatedly with dry pentane until the washings remained colorless. Trace amounts of ferrocene (ca. 4−5%) were recovered from the washings and identified by solution ^1H NMR spectroscopy. Elemental analysis indicated 8.28 wt % Fe and was consistent with incorporation of Fe(η-C_5H_4)$_2$SiMe$_2$ units.

Synthesis of MCM-41/Fe(C_5Me_4)$_2$SiMe$_2$ (2). [Fe(η-C_5Me_4)$_2$SiMe$_2$] was synthesized according to published procedures.[23] MCM-41 (250 mg) was heated to 150 °C under a dynamic vacuum of 10^{-4} Torr for 6 h. [Fe(η-C_5Me_4)$_2$SiMe$_2$] (300 mg) was dissolved in dry pentane (40 mL) and transferred onto the MCM-41. The slurry was stirred at room temperature for 24 h under N_2. The slurry was allowed to settle and the supernatant decanted. The product, a pale orange powder, was washed repeatedly with dry pentane, until the washings remained colorless, and then dried in vacuo. Elemental analysis indicated 3.44 wt % Fe and was consistent with incorporation of Fe(η-C_5Me_4)$_2$SiMe$_2$ units.

Synthesis of FSM-16/Fe(η-C_9Me_6)(η-C_5H_4)SiMe$_2$ (3). [Fe(η-C_9Me_6)(η-C_5H_4)SiMe$_2$] was synthesized by reaction of 1 equiv of dilithiocyclopentadienyl(hexamethylindenyl)dimethylsilane with $FeCl_2$·1.5THF.[24] FSM-16 (200 mg) was heated to 130 °C at 10^{-2} Torr for 3 h and then at 3×10^{-5} Torr for 5 h. [Fe(η-C_9Me_6)(η-C_5H_4)SiMe$_2$] (180 mg) was dissolved in dry pentane (40 mL) and added to the FSM-16 under N_2. The suspension was stirred at 45 °C overnight. After 24 h a purple solid was recovered, washed repeatedly with pentane, and dried in vacuo. Elemental analysis indicated 5.44 wt % Fe. The pentane washings contained trace amounts of the starting material [Fe(η-C_9Me_6)(η-C_5H_4)SiMe$_2$] identified by solution ^1H NMR spectroscopy.

Synthesis of Octamethylferrocenyl-Functionalized MCM-41 and FSM-16. Samples of MCM-41 and FSM-16 were dried in vacuo (10^{-4} Torr) for 5 h at room temperature and then heated to 120 °C for 3−4 h. [Fe(η-C_5Me_4OH)(η-C_5Me_4H)][25] (200 mg) was dissolved in diethyl ether (10 mL). Acetic anhydride (0.2 mL) was added through a septum followed by HBF_4·Et_2O (0.2 mL, 85%) by syringe. An orange precipitate formed immediately. The solid was recovered by filtration and washed with Et_2O:pentane (2:1 ratio, 3×30 mL), and the orange/brown solid was dried in vacuo. The product was then dissolved in dry acetone (30 mL), forming a dark red solution which was transferred immediately onto the mesoporous silicate. In each case pale green, air-stable powders were obtained.

Results and Discussion

Synthesis of Fe(η-C_5H_4)$_2$SiMe$_2$-Modified MCM-41 (1). Addition of a pentane solution of an excess of (1,1′-ferrocenediyl)dimethylsilane, [Fe(η-C_5H_4)$_2$SiMe$_2$], to a dehydrated sample of MCM-41 results in functionalization of the mesoporous host via a ring-opening reaction initiated by the nucleophilic ≡Si−*O*H sites within the mesopores. The reaction is shown schematically in Figure 2.

The orange air-stable solid obtained after washing with pentane to remove any soluble species was then dried in vacuo. Elemental analysis indicates that the material contains 8.3 wt % Fe (ca. 40 wt % organometallic). This is equivalent to combining 200 mg of host with 130 mg of guest (2.7 mmol/g of host) and is consistent with a coverage of ferrocenyl units of 3.2×10^{-10} mol cm^{-2}. The X-ray powder diffraction pattern of pristine MCM-41 and **1** are shown in parts a and b of Figure 3, respectively. For the pristine MCM-41, the observed reflections can be indexed on a hexagonal unit cell ($a = 2d_{100}/\sqrt{3} = 43.9$ Å). While the X-ray powder diffraction pattern of **1** indicates a slightly lower crystallinity than for the unmodified MCM-41, the observation of the strongest low-angle reflection ($d = 38.0$ Å, indexed as the 100 reflection) is consistent with reten-

(22) Kresge, C. T.; Leonowicz, M. E.; Roth, W. J.; Vartuli, J. C.; Beck, J. S. *Nature* **1992**, *359*, 710−712.

(23) Pudelski, J. K.; Foucher, D. A.; Honeyman, C. H.; Lough, A. J.; Manners, I.; Barlow, S.; O'Hare, D. *Organometallics* **1995**, *14*, 2470.

(24) Tudor, J.; Barlow, S.; Payne, B. R.; O'Hare, D.; Nguyen, P.; Manners, I. Manuscript in preparation.

(25) Zou, C.; Wrighton, M. S. *J. Am. Chem. Soc.* **1990**, *112*, 7578−7584.

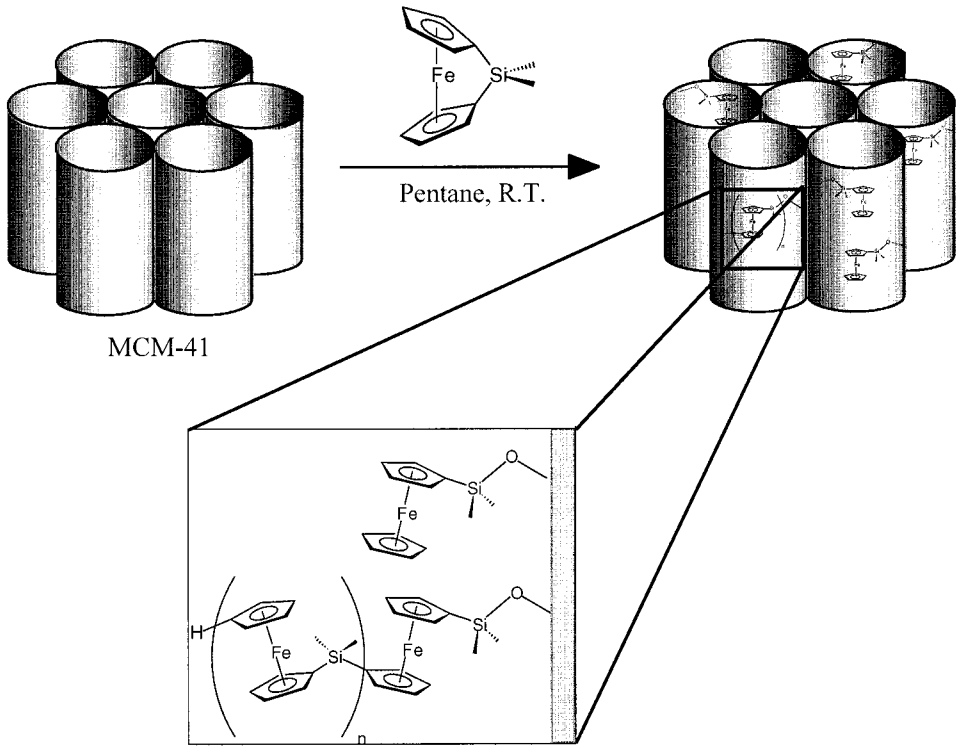

Figure 2. Schematic of the ring-opening reaction of a [1]ferrocenophane on the walls of a mesoporous silicate.

tion of the hexagonal mesoporous structure. Retention of the structure of the host was confirmed by XRD for all subsequent reactions.

To investigate how the ferrocenyl units are bonded to the mesoporous silicate, we have studied this material using solid-state ^{13}C and ^{29}Si NMR and X-ray absorption spectroscopy.

Solid-State NMR Spectroscopic Studies. The room-temperature solid-state cross polarization magic angle spinning (CP MAS) ^{29}Si NMR spectrum of **1** (Figure 4a) exhibited four resonances. The two low-frequency resonances at $\delta = -101.1$ and -108.0 are assigned as two convoluted broad peaks representative of the silica framework, consisting mainly of Q_3 and Q_4 units with the presence of a very little Q_2 at $\delta = -90.8$ [Q_n is defined as $Si(OSi)_n(OH)_{4-n}$]. Comparison with the ^{29}Si NMR spectrum of the original mesoporous silicate showed that the intensity of Q_2 and Q_3 had decreased significantly (Figure 5). This was corroborated by a reduction the intensity of the ν(OH) absorption at 3745 cm^{-1} in the IR spectrum, an absorption band associated with isolated OH groups on the silica surface.[26]

The resonance at $\delta = 7.0$ is assigned as a Si−O−*Si*Me_2Fc moiety (Fc = ferrocenyl group), in accordance with previously reported chemical shifts for similar species.[2,27] The remaining sharp resonance at $\delta = -6.5$ has a longer relaxation time than the other resonances and hence the effects of a slightly truncated FID are observed for the acquisition time employed. This resonance is assigned to the bridging silicon atoms in small oligomers of ferrocenylsilane, the first unit of which is bound to the channel wall, as shown schematically in Figure 2. The chemical shift is in excellent agreement

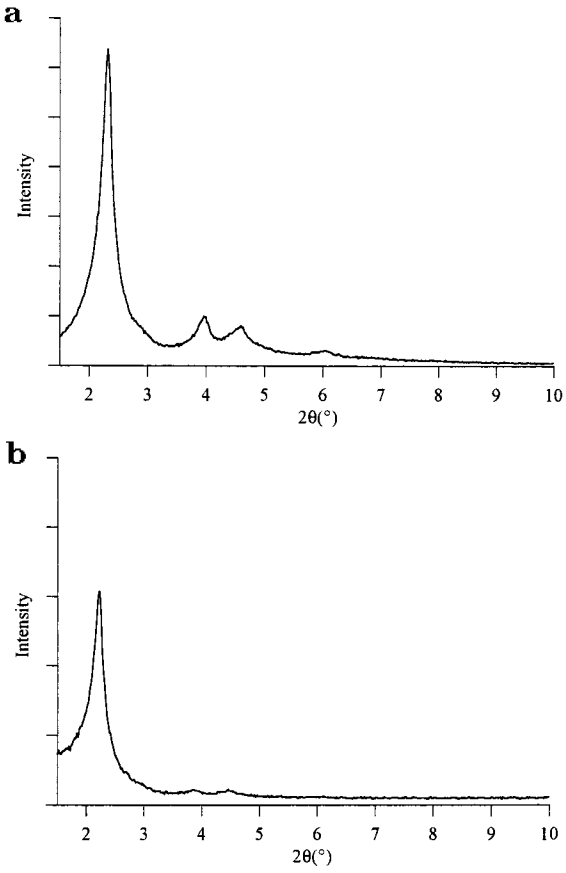

Figure 3. X-ray powder diffraction patterns of (a) MCM-41 and (b) **1**. In both cases $d_{100} = 38.0$ Å (lattice parameter $a = 43.9$ Å)

with the value of −6.4 ppm reported for poly(ferrocenylsilane) in C_6D_6.[15] The lower line width is consistent with the greater motional averaging likely to be experienced by such a Si atom which would result in a lower

(26) Iler, R. K. *The Chemistry of Silica*. J. Wiley and Sons, Inc. **1979**.
(27) Sindorf, D. W.; Maciel, G. E. *J. Am. Chem. Soc.* **1983**, *105*, 3767−3776.

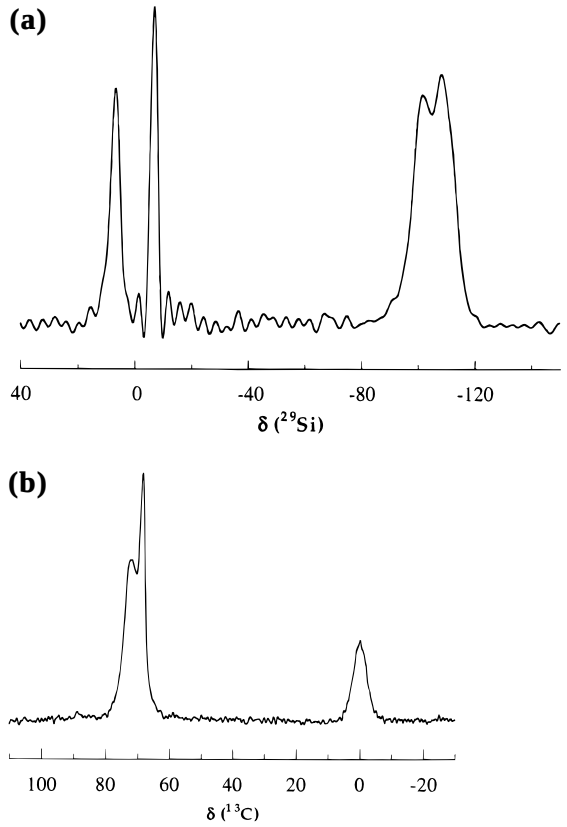

Figure 4. Room-temperature, solid-state CP MAS NMR spectra of **1**: (a)^{29}Si, spinning rate and contact time of 2.47 kHz and 2.0 ms and (b) ^{13}C with spinning rate and contact time of 2.66 kHz and 1.0 ms.

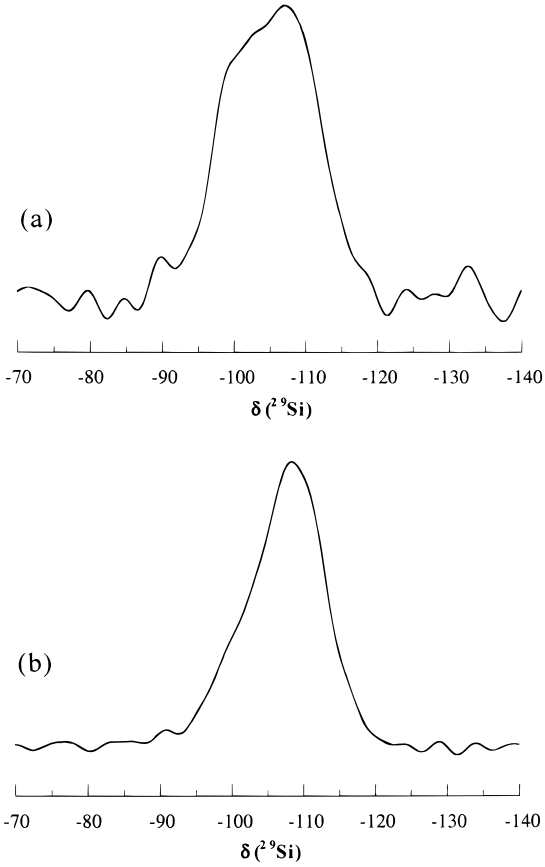

Figure 5. Room-temperature ^{29}Si MAS NMR spectra of (a) MCM-41 and (b) **1**.

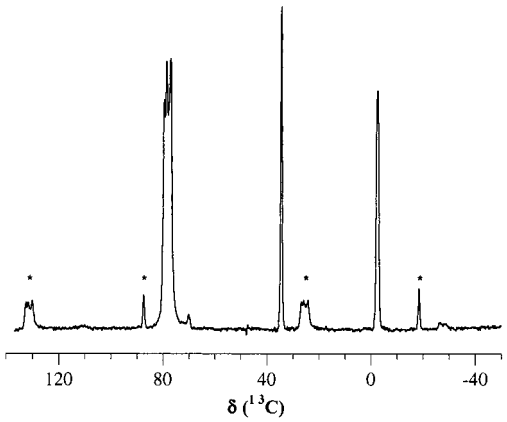

Figure 6. ^{13}C CP MAS NMR spectrum of (1,1′-ferrocenediyl)-dimethylsilane. Acquisition time, 0.02 s; recycle delay, 4 s; contact time, 1.2 ms; spinning rate, 2.66 kHz. Spinning sidebands are marked with an asterisk.

chemical shift dispersion. Integration of the two μ-*Si*Me$_2$ resonances over a range of contact times gave approximately constant intensity ratios of 3 ± 0.2 ($\delta = -6.5$): 4 ± 0.2 ($\delta = 7.0$), suggesting that the ratio of wall-tethered ferrocenyl groups to those present in oligomeric chains is in the ratio 4:3. It is reasonable to assume that magnetization transfer from the two directly bonded methyl groups is largely responsible for roughly equivalent cross polarization to the two chemically and magnetically inequivalent ^{29}Si nuclei. Hence, a molecular formula which is consistent with both the elemental microanalytical data and the solid-state NMR spectroscopic studies is $(SiO_2)_{11}O_3SiO\{Fe(\eta\text{-}C_5H_4)(\eta\text{-}C_5H_4\text{-}SiMe_2)\}\{Fe(\eta\text{-}C_5H_4)(\eta\text{-}C_5H_4SiMe_2)\}_m$ where $m = 0.75$. If it is assumed that all the available surface silanol sites of the host react, this formula suggests that 1 in 12 silicon atoms possessed the $-$OH group (to the low end of the range of previously calculated values).[28] The ^{29}Si CP MAS NMR spectrum still exhibits a strong resonance attributable to Q_3 sites. The ^{29}Si MAS NMR shows a decrease in the Q_3/Q_4 ratio of approximately 40%. It is clear that a large number of Q_3 silicon atoms still exist in the composite material. These silanol groups may be contained within the wall framework and therefore sequestered from electrophilic attack. In addition, steric crowding of the guest may prevent reaction with the surface silanol sites available.

The room-temperature ^{13}C CP MAS NMR spectrum of **1** (Figure 4b) exhibits three broad resonances, all of which are much broader than those of the parent [1]-ferrocenophanes. We attribute the increased line widths to the range of chemically different environments in which the molecules are located, giving rise to an envelope of peaks with very similar chemical shifts (chemical shift dispersion). The sample was cooled to 170 K, but no changes were observed in the spectrum. The isotropic chemical shifts are at $\delta = 72.1$, 68.6, and -0.1 with $\nu_{1/2}$ values of ca. 234, 105, and 220 Hz, respectively, cf. [Fe(η-C$_5$H$_4$)$_2$SiMe$_2$] (Figure 6): 180.7 Hz ($\delta = 77-79.5$, C$_5$H$_4$), 30.3 Hz ($\delta = 34.4$, C$_{ipso}-$Si) and 58.3 Hz ($\delta = -2.5$, CH$_3$).

(28) Feuston, B. P.; Higgins, J. B. *J. Phys. Chem.* **1994**, *98*, 4459–4462.

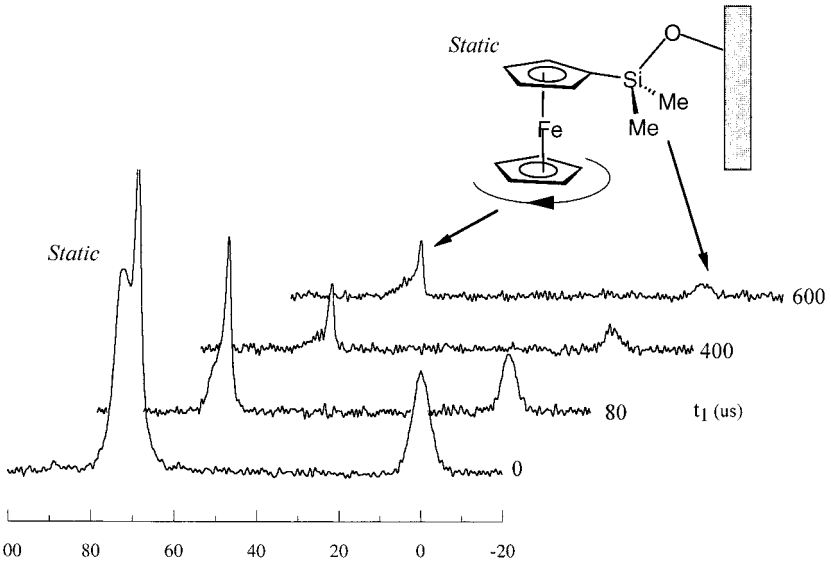

Figure 7. Conventional cross polarization ($t_1 = 0$) and selected dipolar dephasing spectra of **1**.

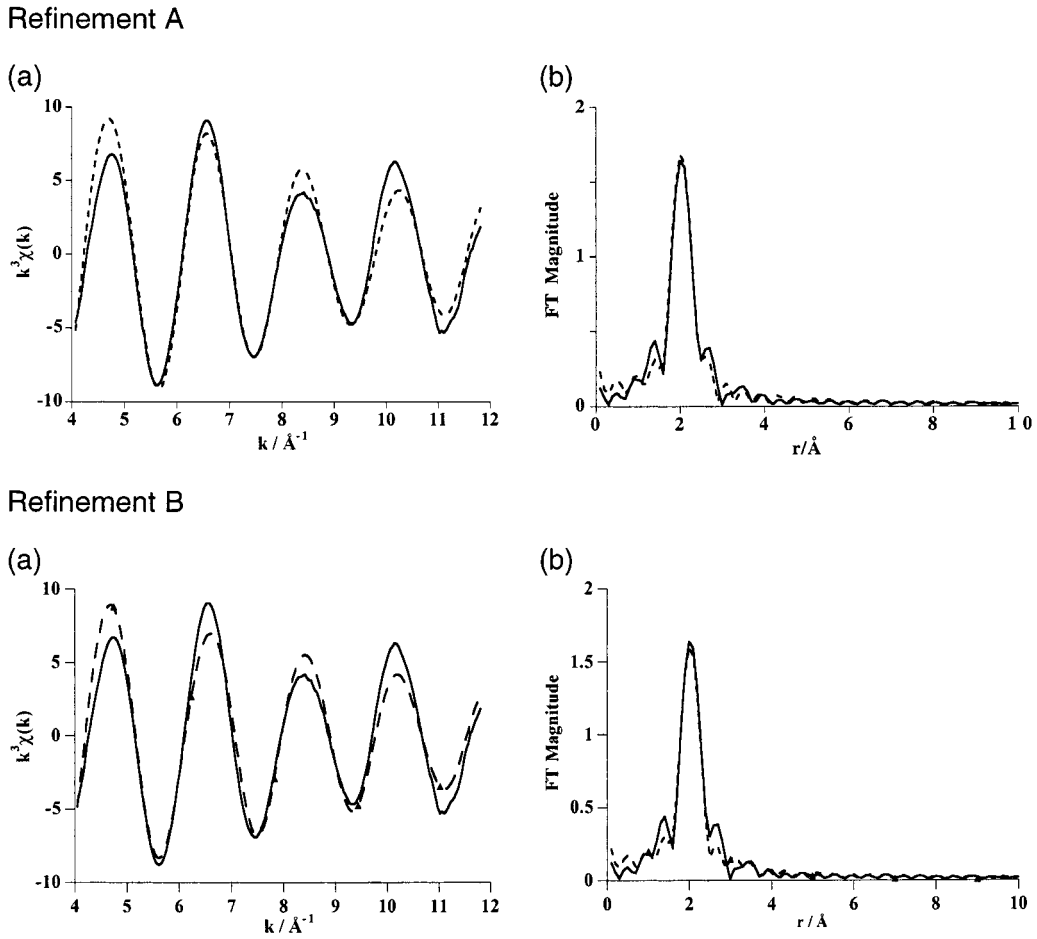

Figure 8. (a) Fe K-edge k^3-weighted transmission EXAFS spectrum and (b) Fourier transform of **1** [(—) experiment; (- - -) curved wave theory]. The structural parameters obtained are given in Table 1; refinement A is the best fit and refinement B includes the Si atom as the second shell.

The resonance at $\delta = -0.1$ (Figure 4b) is assigned to all Si*C*H$_3$ groups, whether wall-grafted or bridging ferrocenyl units (expected chemical shifts of around $\delta = 0.4$ and -0.5 respectively, Figure 2). The high-frequency resonances are attributed to the cyclopentadienyl carbon atoms of ferrocene. The sharper resonance at $\delta = 68.6$ is assigned to the unsubstituted η-C$_5$H$_5$ unit. This chemical shift is comparable to that observed for the η-C$_5$H$_5$ carbon atoms following the ring-opening reaction of (1,1′-ferrocenediyl)dimethylsilane with CD$_3$-OD. The absence of spinning sidebands in the spectrum, even at this relatively low spinning speed (2.66 kHz), is typical of η-C$_5$H$_5$ units.

Cross polarization and dipolar dephasing techniques[29] were employed to aid in the assignment of the ^{13}C CP MAS NMR spectrum. These experiments indicated that

Table 1. EXAFS Structural Parameters for 1 (refinements A, B, and C) and Octamethyl(ferrocenyl)-modified MCM-41 (refinement D)

refinement	shell	scattering atom	N^a	r (Å)[a]	$2\sigma^2$ (Å^2)[b]	R (%)[c]
A	1	C	10	2.045(2)	0.0073(7)	21.8
	2	C	2	2.555(6)	0.0098(4)	
B	1	C	10	2.045(2)	0.0073(3)	26.4
	2	Si	1	3.508(4)	0.015(7)	
C	1	C	10	2.045(3)	0.0074(3)	26.8
D[d]	1	C	10	2.101(4)	0.0075(4)	32.3
	2	C	9	3.207(12)	0.021(4)	

[a] N = coordination number, r = interatomic distance. Standard deviations are in parentheses. [b] Debye−Waller factor; σ is the root-mean-square deviation of the interatomic distance about r. [c] R is the statistical R factor. [d] Fluorescence EXAFS data.

the broad peak at $\delta = 72.1$ exhibited rapid dephasing relative to its neighbors (Figure 7), and so we assign this signal to the CH groups of the cyclopentadienyl ring grafted to the walls. Dephasing was slower for the neighboring signal at $\delta = 68.6$, indicating an attenuated $^{13}C-^{1}H$ dipolar coupling, presumably a result of greater motional freedom in the form of ring rotation.

Fe K-Edge EXAFS Spectroscopic Studies. X-ray absorption fine structure (XAFS) spectroscopy is a proven technique in the investigation of crystallographically disordered systems.[30] The extended X-ray absorption fine structure (EXAFS) study probes the short range order around a specific element. Analysis of the data can yield the local coordination numbers, types of backscattering atoms, and accurate absorber−backscatterer distances. The use of XAFS spectroscopy in the investigation of host−guest systems has been demonstrated previously. For example, the coordination and oxidation states of metal centers were characterized by XAFS spectroscopy in chromia-pillared smectite clays[31] and double layered hydroxides intercalated with polyoxometalate anions.[32] EXAFS has also been used in the study of surface organometallic chemistry on oxide supports.[30]

The Fe K-edge EXAFS spectrum of **1** was recorded on Station 8.1 at the SRS Daresbury Laboratory, UK. The data analysis was initially conducted by postulating a model of ferrocene for the Fe center and hence selecting a single shell (coordination sphere) of 10 carbon atoms. Refinement gave an average Fe−C bond distance of 2.045(3) Å, which was comparable to that observed in crystals of ferrocene. The observed and best fits to the model are shown in Figure 8 (using standard scattering treatment of the EXAFS data),[33] and the parameters are given in Table 1.

The best fit was achieved with an additional second shell of two carbon atoms. If this shell was real it would arise from neighboring rather than bonding carbon atoms, such as the methyl groups attached to the silicon atoms. Inspection of crystallographic data from small oligomers of poly(ferrocenylsilane) reveal that the nonbonded distances for Fe-*Si* and Fe−(*C*H$_3$)Si are 3.50−3.54 and 3.96−4.29 Å, respectively.[16,34] A model that included a Si atom in the second shell would therefore appear to be more reasonable. Although we performed an additional refinement (Table 1, refinement B) with a second shell containing only a Si atom (allowed to refine at around 3.5 Å), the theoretical fit is not as good. When this is compared to a refinement based on a single shell of 10 carbon atoms (Table 1, refinement C), the spectra and R factors were very similar. The statistical probability of the additional shell being real (tested using the STAT command within EXCURV92 program which employs the Joyner test)[33] was calculated to be at the 1% significance level. Hence, there is not enough evidence to verify the reliability of assignments to the second shell. They do, however, demonstrate the ability of EXAFS to characterize the disordered guest species present within an ordered host and confirm that the ferrocenyl fragments remain intact within the silicate framework.

Table 2. ^{13}C Chemical Shifts Observed in the CP MAS NMR Spectrum of 3 and the Solution NMR Spectrum in C_6D_6 (not all shifts are given) of Fe(η-C$_9$Me$_6$H)(η-C$_5$H$_4$Si(OMe)Me$_2$

^{13}C chemical shift (δ)		
3	methanolysis product[a]	assignment[b]
0.3	−1.7, −1.6	Si*C*H$_3$
15.4	13.9−16.9	Ind′ *C*H$_3$
	50.0	*C*H$_3$−OSi
62.2	61.6	Ind′ *C*H
68.6		Cp *C*H
70.5	70.2	Cp C_{ipso}-Si
75.6	75.8	Ind′ quaternary
86.2	86.5, 87.6	Ind′ quaternary
129.7	129.1−131.3	Ind′ quaternary

[a] (Fe(η-C$_9$Me$_6$H)(η-C$_5$H$_4$)Si(OMe)Me$_2$. [b] Ind′ = indenyl. Cp = cyclopentadienyl.

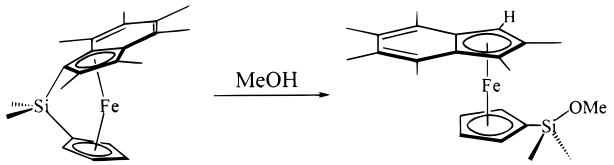

Figure 9. Methanolysis reaction of [Fe(η-C$_9$Me$_6$)(η-C$_5$H$_4$)-SiMe$_2$]. The direction of ring opening was determined by solution ^{1}H and ^{13}C{H} NMR spectroscopy.

Synthesis of Fe(η-C$_5$Me$_4$)$_2$SiMe$_2$-Modified MCM-41 (2). In an analogous manner to the nonmethylated derivative [Fe(η-C$_5$H$_4$)$_2$SiMe$_2$], the addition of a pentane solution of [Fe(η-C$_5$Me$_4$)$_2$SiMe$_2$] (an excess) to a dehydrated sample of MCM-41 affords, after workup, a pale

(29) Alemany, L. B.; Grant, D. M.; Alger, T. D.; Pugmire, R. J. *J. Am. Chem. Soc.* **1983**, *105*, 6697−6704.
(30) Evans, J. *Chem. Soc. Rev.* **1997**, *26*, 11−19.
(31) Corker, J. M.; Evans, J.; Rummey, J. M. *Mater. Chem. Phys.* **1991**, *29*, 201.
(32) Evans, J.; Pillinger, M.; Zhang, J. J. *J. Chem. Soc., Dalton Trans.* **1996**, 2963−2974.
(33) Binsted, N.; Campell, J. W.; Gurman, S. J.; Stephenson, P. *EXCURV92−Program*; SERC Daresbury Labs: Warrington, 1992.
(34) Pannell, K. H.; Dementiev, V. V.; Li, H.; Cervantes-Lee, F.; Nguyen, N. T.; Diaz, A. F. *Organometallics* **1994**, *13*, 3644.

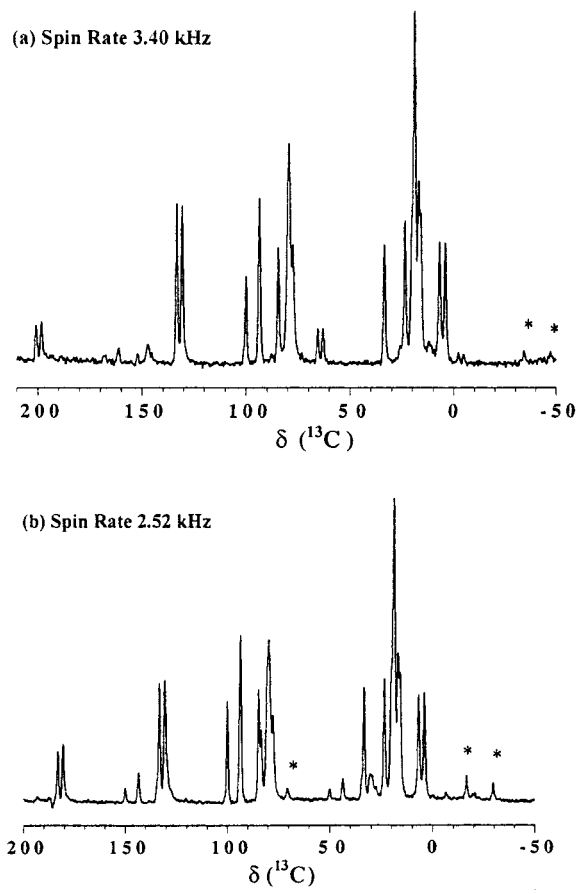

Figure 10. Room-temperature, solid-state ^{13}C CP MAS NMR spectra of [Fe(η-C_9Me_6)(η-C_5H_4)$SiMe_2$]; spin rate, 3.3 kHz; acquisition time, 0.02 s; recycle delay, 4 s; contact time, 1.2 ms; 7000 scans.

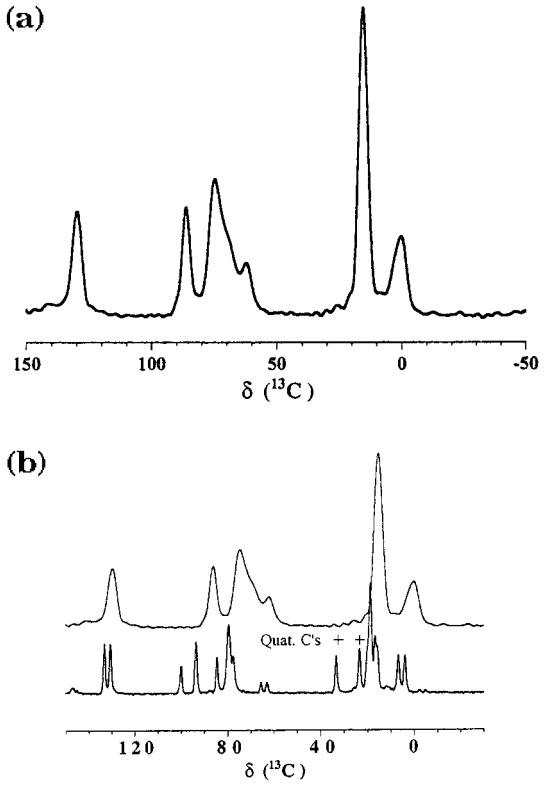

Figure 11. Room-temperature, solid-state ^{13}C CP MAS NMR spectrum of (a) **3** (spin rate, 3.3 kHz; acquisition time, 0.01 s; contact time, 1.2 ms) and (b) viewed above the ^{13}C NMR CP MAS spectrum of the unreacted [Fe(η-C_9Me_6)(η-C_5H_4)$SiMe_2$].

orange microcrystalline solid. Elemental analysis indicated that the material contains 3.4 wt % Fe (ca. 21 wt % organometallic). Unlike its nonmethylated analogue, this product is air-sensitive and adopts a green color after exposure to air for more than 1 h, presumably the result of oxidation of the Fe center.

The room-temperature ^{13}C CP MAS NMR spectrum of **2** exhibited resonances attributable to the ring quaternary (δ = 84 and 80), the C_5Me_4H methine (δ = 70), the ring methyl (δ = 10), and the $SiMe_2$ (δ = 0) carbon environments. The absence of any low-frequency resonances at ca. δ = 30 confirmed the successful completion of the ring-opening reaction and was consistent with the grafting of the organometallic moiety onto the mesoporous host.

The ^{29}Si MAS NMR spectrum of **2** exhibited two broad convoluted resonances at δ = −100.4 and −109.4 attributable to Q_3 and Q_4 units of the silica framework. A further three resonances were observed at δ = 9.8, −19.0, and −22.3. The high-frequency resonance is assigned as a Si−O−*Si*Me_2Fc moiety by analogy with Fe(η-C_5H_4)$_2$$SiMe_2$/MCM-41. We attribute the two resonances at lower frequency (of approximately equal intensity) to bridging $SiMe_2$ units between octamethylferrocenyl moieties. The observation of two resonances for this Si environment most likely arises from oligomeric units of differing lengths.

Synthesis of Fe(η-C_9Me_6)(η-C_5H_4)$SiMe_2$-Modified FSM-16 (3). The mixed-ring [1]ferrocenophane, [Fe(η-C_9Me_6)(η-C_5H_4)$SiMe_2$], can be prepared by reaction of dilithio(cyclopentadienyl)(hexamethylindenyl)dimethylsilane with $FeCl_2$·1.5THF in THF.[24] To confirm its potential as a grafting agent (i.e. the susceptibility of the molecule to nucleophilic attack), a methanolysis reaction was performed by treatment of a THF solution of the compound with excess CH_3OH. Solution ^1H and ^{13}C NMR spectroscopy (Table 2) and mass spectrometry confirmed bond scission and the formation of a single ring-opened product (Figure 9). The product suggests that the mechanism of the reaction involves protonation of the *ipso*-carbon before nucleophilic attack of the silicon. We were interested to see if it would also exhibit regioselective ring opening within the mesoporous silicate.

Addition of a warm pentane solution of the mixed ring [1]ferrocenophane [Fe(η-C_9Me_6)(η-C_5H_4)$SiMe_2$] to a dehydrated sample of FSM-16 again results in irreversible immobilization within the mesopores. Washing with pentane removed a residual quantity of unreacted [1]-ferrocenophane. The product, a purple, air-sensitive solid, was dried in vacuo. Elemental microanalysis indicated that the material contains ca. 5.4 wt % Fe. X-ray powder diffraction indicated that the material was slightly less crystalline than the original hexagonal FSM-16.

We initially recorded the solid-state ^{13}C NMR spectrum of [Fe(η-C_9Me_6)(η-C_5H_4)$SiMe_2$] to assign the resonances and to allow a comparison with the final modified mesoporous silicate. The two sets of ^{13}C CP MAS NMR spectra (acquired at different MAS rates) are shown in Figure 10.

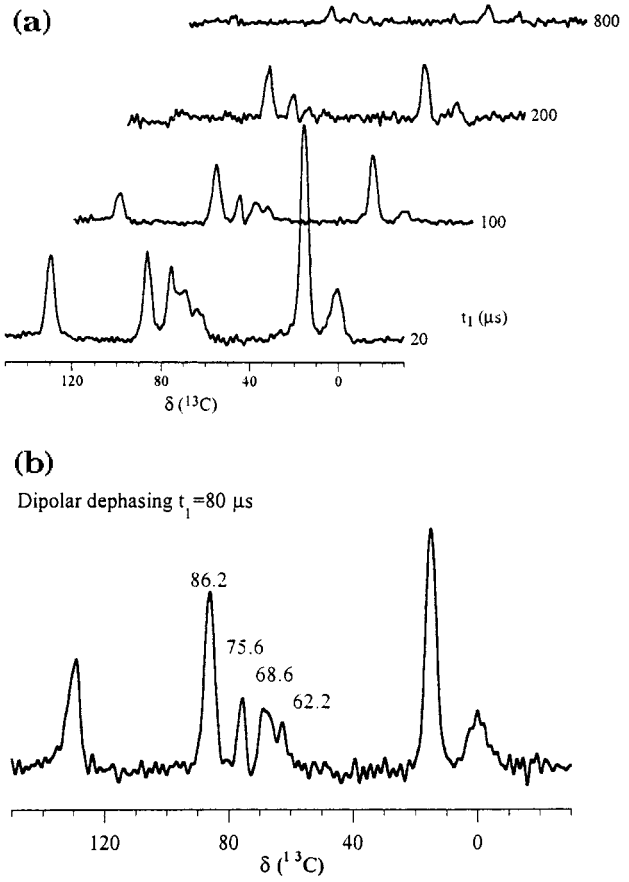

Figure 12. Solid-state ^{13}C CP MAS NMR dipolar dephasing experiments of **3**: (a) a series of spectra at successive dephasing times, t_1, (b) spectrum at t_1 = 80 ms with chemical shifts of the group of resonances between δ = 60 and 90 ppm.

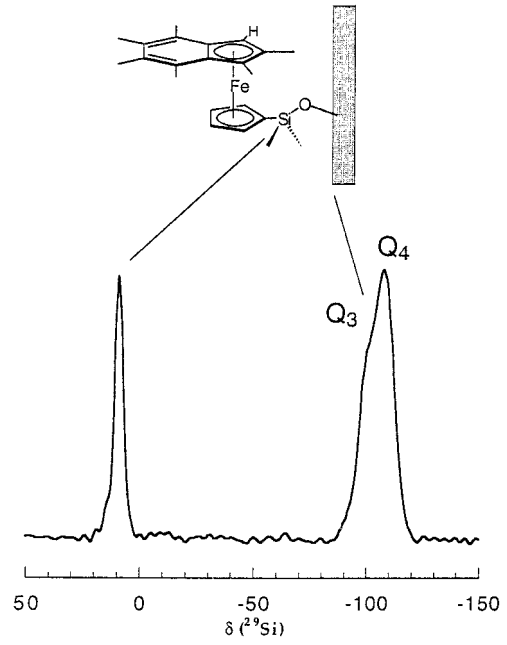

Figure 13. Room-temperature, solid-state ^{29}Si CP MAS NMR spectrum of **3** together with a schematic (top) to illustrate the major ring-opened product and the assignment of the silicon resonances.

Of all the resonances observed in the region $\delta = 0-50$, only those at δ = 33.4 and 20.2 exhibit spinning sidebands (marked with an asterisk in each of the spectra). The larger chemical shift anisotropy associated with these two resonances precludes their assignment as methyl groups. They are therefore assigned to the ipso carbons of the C_5H_4 and C_9Me_6 (Ind′) rings, respectively. Such low-frequency chemical shifts have previously been observed for, and unambiguously assigned to, the ipso carbon atoms of metallocenophanes: the low-frequency shift is characteristic of the high strain present in these molecules. The absence of such low-frequency resonances provides evidence important in determining the success or failure of ring-opening within the host.[23,35]

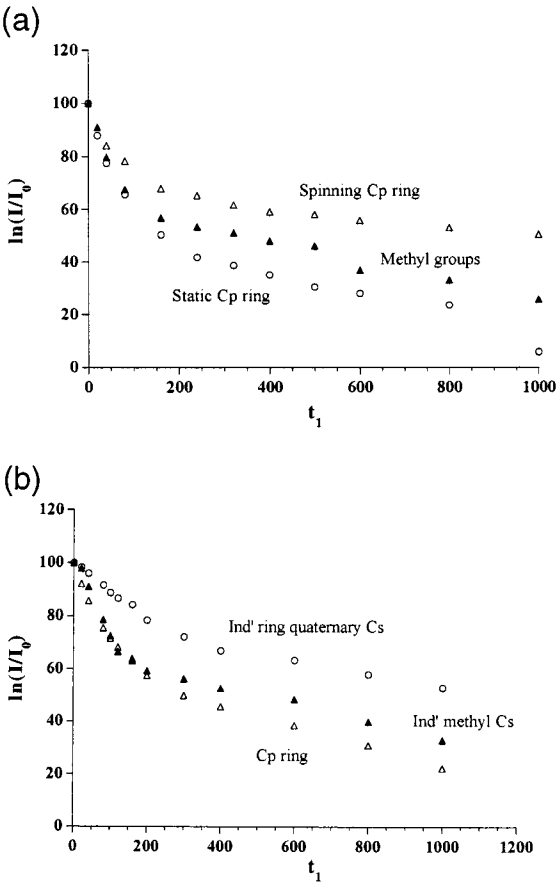

Figure 14. Plots of ln(I/I_0) vs t_1 for selected carbons in (a) Fe(η-C_5H_4)$_2$SiMe$_2$-modified MCM-41 (**1**) and (b) Fe(η-C_9Me_6)-(η-C_5H_4)SiMe$_2$-modified FSM-16 (**3**).

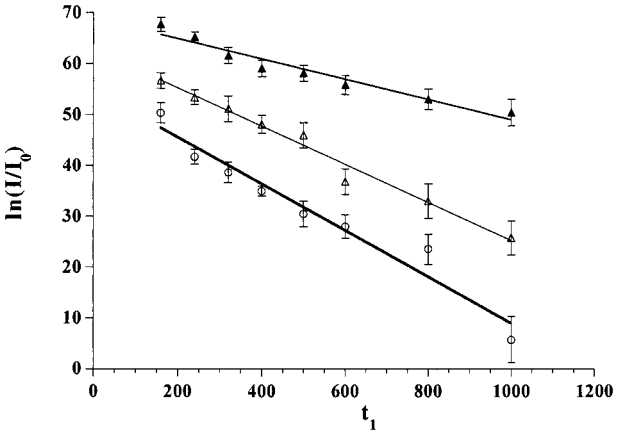

Figure 15. Plot of the expanded region of Figure 13, showing linear fits to plots of ln(I/I_0) vs t_1 for the η-C_5H_5 ring (triangles), the methyl groups (filled triangles), and the wall-tethered C_5H_4 ring (circles) present in **1**.

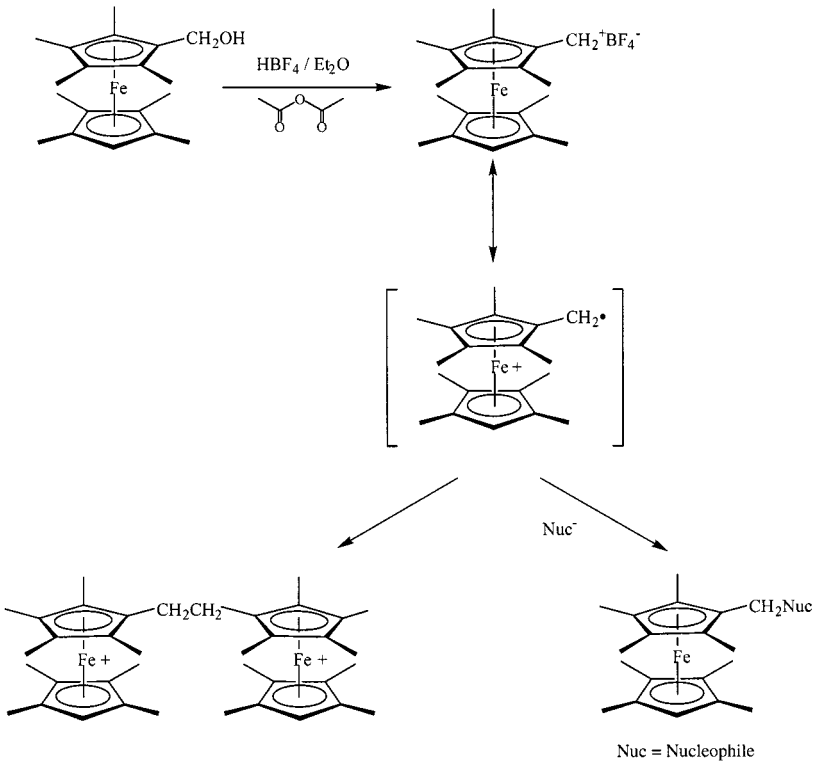

Figure 16. Synthesis of the octamethyl(ferrocenyl) carbocation and its reactivity (adapted from Zou et al.)[25]

Table 3. Approximate Time (ms) for the Carbon Signal Intensity to Decay by 50%, and the Decay Rate (exponential decay constant, T_2') for Functional Groups in Organic Compounds, Fe(η-C_5H_4)$_2$SiMe$_2$-Modified MCM-41 (1) and Fe(η-C_9Me_6)(η-C_5H_4)SiMe$_2$-modified FSM-16 (3)

functional group[a]	estd 50% decay (ms)	calcd T_2' values (ms)
Organic Compounds[29]		
CH_2	14−33	12−29
CH	20−40	15−32
non-*tert*-butyl CH_3	40−92	50−121
nonprotonated sp^2	50−175	75−218
1 (δ in parentheses)		
Cp CH (68.6)	37	50
Cp CH (72.1)	30	22
Si CH_3 (−0.1)	32	37
3 (δ in parentheses)		
Cp CH (68.6)	40	24
Ind′ C (75.6)	33	30
Ind′ C (86.2)	140	39
Ind′ CH_3(15.4)	60	30
Si−CH_3(0.3)	52	38

[a] Ind′ = indenyl. Cp = cyclopentadienyl.

The solid-state ^{13}C CP MAS NMR spectrum of **3** is shown in Figure 11. The line widths are again much broader than those observed for the crystalline solid and is once more attributed to chemical shift dispersion. For example, one of the methyl resonances of [Fe(η-C_9Me_6)(η-C_5H_4)SiMe$_2$] at δ = 18.9 has a $\nu_{1/2}$ value of 52 Hz, while all the methyl resonances for the modified-silicate collectively form an envelope of peaks with an average chemical shift of δ = 15.4 and $\nu_{1/2}$ value of 217 Hz. The absence of resonances for the ipso carbons of the C_5H_4 and Ind′ rings at very low frequency (now occurring within the envelope of peaks at δ = 60−90) confirmed the successful ring opening of [Fe(η-C_9Me_6)(η-C_5H_4)-SiMe$_2$] on the walls of the mesoporous silicate. In an attempt to resolve the resonances in the region δ = 60−90, dipolar dephasing experiments were carried out, allowing a more precise determination of chemical shift values (Figure 12).

The peak at δ = 62.2 is typical for a ^{13}C−H resonance in an indenyl ring and occurs to significantly lower frequency than observed for C_5H_5−ferrocenyl derivatives. In the $^{13}C\{^1H\}$ NMR spectrum of the methanolysis product, Fe(η-C_9Me_6H)(η-$C_5H_4Si(OMe)Me_2$), a resonance at a similar chemical shift was observed, confirming that ring-opening results in the silicon moiety being located on the cyclopentadienyl ring. The intensity of the resonance at δ = 86.2 decays very slowly relative to its counterparts, indicating that this resonance is due to one or more quaternary carbons.

The room-temperature solid-state ^{29}Si CP MAS NMR spectrum of **3** is shown in Figure 12. Unlike for Fe(C_5H_4)$_2$SiMe$_2$-modified MCM-41 (**1**), only three resonances are observed. The two peaks in close proximity at δ = −100.3 and −107.2 are assigned as two convoluted broad peaks consistent with a Q_3 and Q_4 silica framework. The third isotropic resonance at δ = 9.2 is assigned as the O−Si(Me)$_2$R silicon bridging atom between the wall of the mesoporous silicate and the tethered organometallic species. A series of ^{29}Si CP MAS NMR spectra at differing contact times indicated the presence of a shoulder at δ = 14.0, possibly as a result of a relatively small number of bridging silicon atoms between the wall and the Ind′ ring.

It is therefore concluded that the majority of molecules are tethered to the silicate wall via the cyclopentadienyl ring (Figure 13) with a trace amount of ring-opening in the opposite direction. There is no evidence

(35) Finckh, W.; Tang, B.-Z.; Foucher, D. A.; Zamble, D. B.; Ziembinski, R.; Lough, A. J.; Manners, I., *Organometallics* **1993**, 823−829.

of a signal at ca. $\delta = -6.5$, and thus it is concluded that there are no oligomeric units derived from [Fe(η-C_9Me_6)-(η-C_5H_4)$SiMe_2$]. This is in agreement with the observation that TROP reactions did not occur for this ferrocenyl derivative,[36] presumably due to its steric bulk.

Dipolar dephasing experiments were performed over a range of dephasing times on both Fe(η-C_5H_4)$_2SiMe_2$/MCM-41 (**1**) and Fe(η-C_9Me_6)(η-C_5H_4)$SiMe_2$/FSM-16 (**3**) in order to compare the relative signal decay rates of the carbon atoms present. For ^{13}C nuclei weakly coupled to ^1H, a simple exponential decay is expected with a time constant T_2'.[29,37] However, for strong coupling the signal decay is more rapid (typically $t_1 <$ 200 ms). An inspection of the plots of log intensity [ln-(I/I_0)] against dephasing period (t_1, Figure 14) reveals that both strong and weak coupling $^{13}C-^1H$ interactions exist. Despite this, the data in the region $200 \leq t_1 \leq 1000$ (ms) gave a good fit to a straight line of gradient [$(-T_2')^{-1}$] (Figure 15). The derived exponential decay constants are given in Table 3, together with those typically observed for simple organic molecules. A comparison of these data indicate that the observed T_2' values fall broadly within the expected range.

Synthesis of Octamethylferrocene Derivatives of Mesoporous Silicates. Wrighton and co-workers' interest in using electron-rich ferrocene reagents as electrode surface modifiers[38] led to the useful synthetic route to a reactive (octamethylferrocenyl)methyl carbocation.[25] Octamethylferrocene derivatives could then be synthesized via nucleophilic attack on the carbocation.

A freshly prepared (octamethylferrocenyl)methyl carbocation solution was transferred to predried samples of FSM-16 and MCM-41 (heated at 130 °C for 5 h under 3×10^{-5} Torr) in ratios of 2.4 mmol/g of host. In all cases the products obtained were pale green, microcrystalline solids. After washing the green solids with dry acetone, the elemental microanalytical data indicated that loading of the octamethylferrocene units within the mesoporous structure varied between 0.2 wt % and 0.4 wt % Fe. This is significantly lower than the loading obtained using the ring-opening reactions with [Fe(η-C_5R_4)$_2SiMe_2$] (R = H or Me) or [Fe(η-C_9Me_6)(η-C_5H_4)$SiMe_2$]. The green color of the samples suggested that some of the octamethylferrocene centers had been oxidized to ferrocenium species. The solid-state EPR spectrum at 5 K showed a characteristic absorption at $g = 4.39$, which can be assigned to the $g_{||}$ of an octamethylferrocenium ion.

The Fe K-edge EXAFS of samples of octamethylferrocenyl-modified MCM-41 and FSM-16 were recorded on Station 8.1 at the SRS Daresbury Laboratory and were found to be identical for both samples. Due to the low abundance of Fe in the sample, fluorescence EXAFS was the preferred technique. Figure 17 shows the observed and best fit to the model described below, using standard scattering treatment of the EXAFS data.[33] The parameters are given in Table 1 (refinement D).

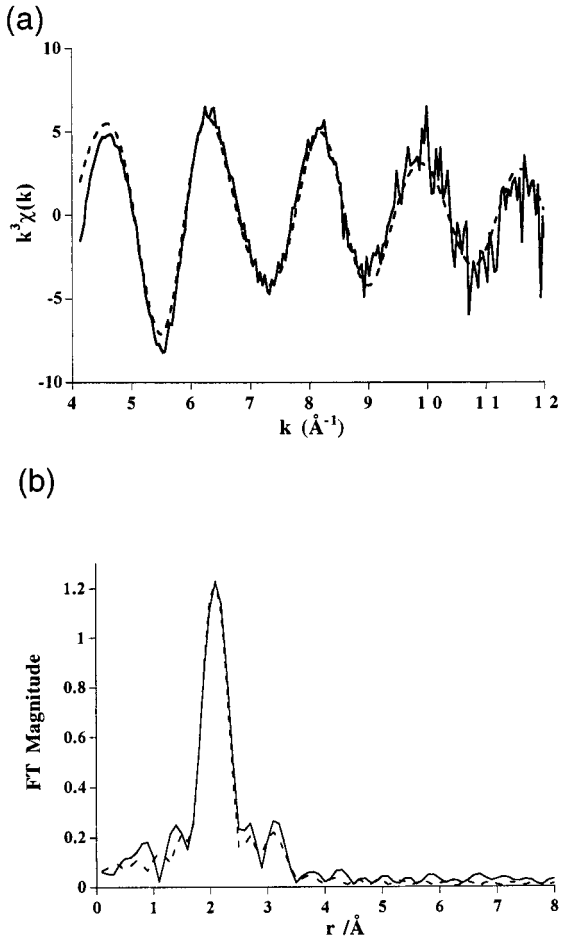

Figure 17. (a) Fe K-edge fluorescence EXAFS spectrum and (b) Fourier transform of octamethyl(ferrocenyl)-modified MCM-41, together with best fit [(—) experiment; given curved wave theory]. The structural parameters obtained are shown in Table 1, refinement D.

The analysis performed was similar to that described above: a model of ferrocene was employed, selecting a single shell (coordination sphere) of 10 carbon atoms. Refinement gave an average Fe—C bond length of 2.101-(4) Å, comparable to those observed in crystals of ring-substituted ferrocenium ions, such as decamethylferrocenium (average Fe—C bond length = 2.095 Å).[39] The best fit was achieved with a second shell of nine carbon atoms at 3.207(12) Å, attributed to backscattering due to the methyl groups and methylene. Fe—CH_3 nonbonded distances derived from crystallographic data for decamethylferrocenium and decamethylferrocene were found to be 3.223 and 3.213 Å respectively,[39,40] in good agreement with the refined distance for the second shell. Since it has been previously established that the (octamethylferrocenyl)methyl carbocation can react with silanol groups on surface silica,[25] single scattering EXAFS analysis has provided adequate evidence for intact (octamethylferrocenyl)methyl units within the mesoporous silicate host, as depicted in Figure 18.

(36) Payne, B.; O'Hare, D.; Nguyen, P.; Manners, I. Unpublished results, 1997.

(37) $I = I_0 \exp(t_1/T_2')$, where I = intensity, I_0 = intensity at $t_1 = 0$ and T_2' is the decay constant.

(38) Wrighton, M. S.; Palazzotto, M. C.; Bocarsly, A. B.; Bolts, J. M.; Fischer, A. B.; Nadjo, L. *J. Am. Chem. Soc.* **1978**, *100*, 7264—7270.

(39) Miller, J. S.; Calabrese, J. C.; Rommelmann, H.; Chittipeddi, S. R.; Zhang, J. H.; Reiff, W. M.; Epstein, A. J. *J. Am. Chem. Soc.* **1987**, *109*, 769.

(40) Freyberg, D. P.; Robbins, J. L.; Raymond, K. N.; Smart, J. C. *J. Am. Chem. Soc.* **1979**, *101*, 892.

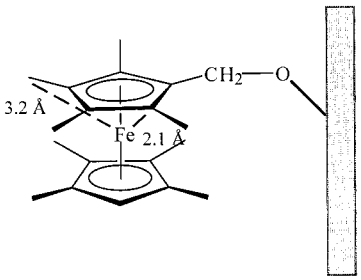

Figure 18. Schematic showing the grafting of an octamethyl-(ferrocenyl) unit to the wall of a mesoporous silicate. The distances (dotted lines) between the Fe−C (C_5H_4) and Fe−C (Me) quoted are those obtained from the EXAFS refinement.

Conclusions

The modification of the pore walls of the mesoporous silicates MCM-41 and FSM-16 has been achieved by treatment of the dehydrated mesoporous silicates with strained [1]ferrocenophanes. The organometallic complexes react with the surface Si−OH (Q_3) giving a C_5R_4−$SiMe_2$−O (R = H or Me) linkage to the silicate surface. These surface-bound ferrocenyl species have been characterized using a number of solid-state NMR and X-ray absorption spectroscopic experiments. The loadings of the Fe (measured as wt %) was in the order [Fe(η-$C_5H_4)_2SiMe_2$] (**1**) > [Fe(η-C_9Me_6)(η-C_5H_4)$SiMe_2$] (**3**) > [Fe(η-$C_5Me_4)_2SiMe_2$]. (**2**). It is expected that higher loadings of **1** would be achieved, given the ease of polymerization of this molecule relative to **2** and **3**. Functionalization of mesoporous silicates using the octamethyl(ferrocenyl) carbocation proved less successful, affording lower loading of the organometallic guest within the mesopores. Partial oxidation of the ferrocene was also observed. Mesoporous solids containing highly methylated rings are redox-active, giving air-sensitive solids in which oxidation of the ferrocenyl to ferrocenium species occurs.

Acknowledgment. The authors would like to thank the EPSRC for financial support and access to the Daresbury Synchrotron Radiation facility. Thanks to Dr. J. Sloan for the transmission electron microscopy of FSM-16 and to Dr. J. F. W. Mosselmans for assistance with the EXAFS. S.O. thanks Dr. M. Simpson and Dr. S. J. Heyes for useful discussions about the NMR.

CM980510G